

Many patients with spinal cord injury (SCI) suffer from severe paralysis<sup>1,2</sup>, possibly because injured axons in the adult mammalian central nervous system (CNS), including those in humans, rarely regenerate<sup>1,2</sup>. Recent findings demonstrate that the regulation of both extracellular and intrinsic factors that affect axon regeneration is essential to recovery from adult CNS neuronal injury<sup>3,4</sup>. Reduction or overexpression of intracellular cell-autonomous regulators promotes axon regrowth<sup>5–11</sup>; however, controlled manipulation of the endogenous expression of these molecules is challenging<sup>8</sup>. Regrettably, current protocols for removing or reducing the extracellular inhibitors do not result in axon regeneration sufficient for complete recovery from SCI.

Chondroitin sulphate (CS), a glycosaminoglycan (GAG) produced mainly by reactive astrocytes and partly by NG2 proteoglycan-positive cells after SCI, is the most widely distributed and most potent inhibitor of axon regeneration<sup>3,5–7,12</sup>. CS degradation resulting from application of chondroitinase ABC (ChABC), a bacterial enzyme, to the injury site promotes some additional axon regeneration<sup>6</sup>. Many practical methods can effectively provide ChABC near injury sites; notably, methods involving viral vector delivery of *ChABC*<sup>13–15</sup> result in more axon sprouting<sup>16</sup> (see reviews<sup>17,18</sup>). In addition, we must

consider treatment alternatives; specifically, we must recognize that CS may be physiologically necessary to minimize the inflammation and limit its area after SCI by inhibiting invasion of macrophages<sup>19,20</sup>. Thus, complete removal of CS may exacerbate, not ameliorate, SCI.

Here we focused on optimizing CS synthesis following SCI. The process of the CS synthesis is very complicated, and more than 10 enzymes participate in CS synthesis<sup>21–23</sup> (Fig. 1a). Notably, heparan sulphate (HS) is also a GAG and a potent promoter of axonal growth, and the first enzymatic step of CS synthesis and of HS synthesis are the same<sup>24</sup>. Therefore, the second step in CS synthesis, catalysed by CS *N*-acetylgalactosaminyltransferase-1 (abbreviated as T1 in this paper), is the first unique and rate-limiting step in CS synthesis; consequently, T1 is tightly regulated because it begins CS-specific polysaccharide chain synthesis<sup>24–28</sup>.

Here we generated T1-knockout (T1KO) mice<sup>29</sup> and induced SCI in these and wild-type (WT) mice to investigate the mechanism of recovery from compression-induced (70 kdyn impact force) SCI. T1KO mice exhibited significantly better recovery from SCI based on locomotor behaviours and histological analysis than did untreated WT or ChABC-treated WT mice. Synthesis of HS, as also upregulated in T1KO mice because expression of HS-synthesis enzymes was induced. Notably, ChABC treatment never induced

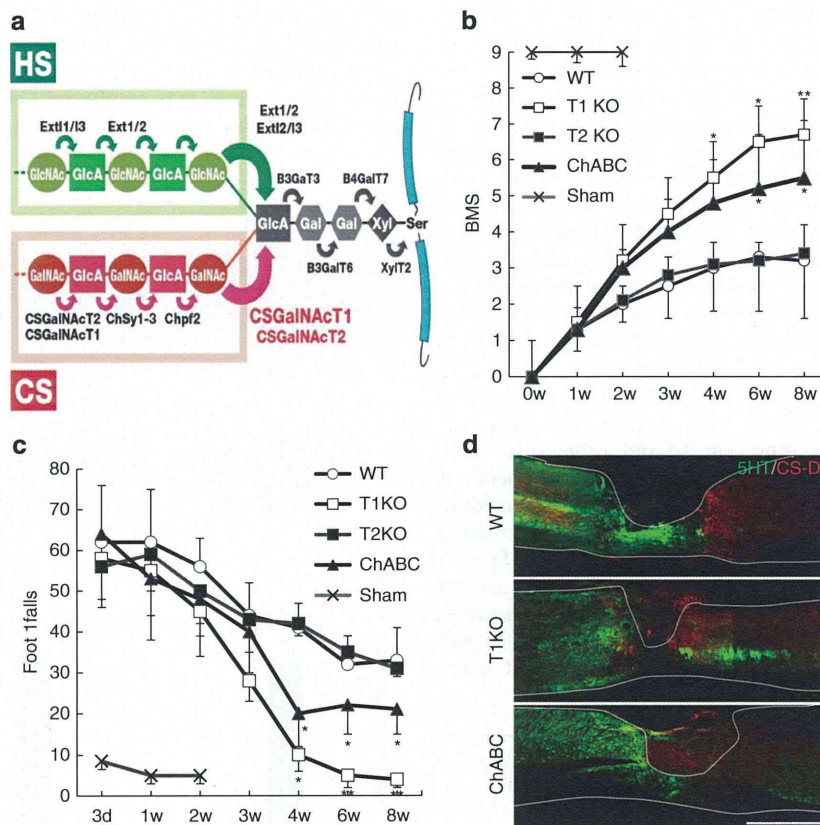


**Figure 1 | T1KO mice recover from SCI more quickly and more completely than WT mice.** (a) Schematic diagram of GAG synthesis. The steps in CS synthesis are as follows: (1) synthesis of the tetrasaccharide linker that is attached to core proteins; (2) attachment of an *N*-acetylgalactosamine (GalNAc) to the linker; (3) addition of glucuronic acid (GlcA) to GalNAc and subsequent polymerization of the disaccharide backbone (GalNAc-GlcA); and (4) sulphation of several sites (a). During CS or HS synthesis T1 transfers GalNAc (CS) to the linker, whereas Ext1/Ext2 transfers GlcNAc (HS). T1 is primarily responsible for the catalysis of the first unique step in CS chain formation<sup>21,22,26,28</sup> (a); therefore, T1 is the most important enzyme for regulation of CS synthesis. See Supplementary Table S2 for a description of enzyme abbreviations. Gal, galactose; GalNAc, *N*-acetylgalactosamine; GlcNAc, *N*-acetylglucosamine; GlcA, glucuronic acid; Xyl, xylose. (b) BMS scores after SCI. (c) Footfall tests after SCI. (b,c) T1KO versus WT and ChABC. *Post hoc* analyses were conducted using the Bonferroni-Dunn test for repeated-measures ANOVA. In b and c, data are expressed as the mean  $\pm$  s.e.m; \* $P < 0.05$ ; \*\* $P < 0.01$  ( $n = 9$ ; ANOVA). (d) Immunohistochemistry of 5HT (+) axon terminals in mice 8 weeks after SCI. 5HT (green) and CS (red). Scale bars, 1 mm.



HS upregulation. Judging from our results and those from two previous reports, an HS-synthesizing enzyme Ext2 satisfies the definition of a potential intrinsic growth regulator in neurons<sup>30,31</sup>. Our results indicate that a single gene, that encodes T1, is a promising therapeutic target for SCI treatment.

## Results

**T1KO recover more rapidly than WT and ChABC-treated mice.** We had focused on optimizing CS synthesis following SCI. However, the formation of a tetrasaccharide linker is notably the first step in both CS and HS biosynthesis, and CS inhibits axonal regrowth, whereas HS promotes it (Fig. 1a). Therefore, the second step in CS and HS synthesis—which is catalysed by T1 and the Ext1-Ext2 heterodimer (Ext1/Ext2), respectively—is the first unique and rate-limiting step in each pathway. These enzymes share a substrate, the tetrasaccharide linker<sup>21</sup>, and they bifurcate GAG synthesis into two alternative pathways<sup>24,26</sup>. Although CS *N*-acetylgalactosaminyltransferase-2 (CSGalNAcT2; abbreviated as T2 in this paper) is a T1 isoform, it has lower enzyme activity than does T1<sup>21,27</sup>.

We focused on reducing T1 activity, via gene knockout, as a potential treatment for SCI. T1KO mice are viable, but they have abnormal bone development and 10% shorter bodies than do WT mice<sup>29</sup> (see Supplementary Fig. S1a–c). Following induced SCI, we examined and compared the recoveries of T1KO, T2-knockout (T2KO), untreated WT and ChABC-treated WT mice. Recovery of motor functions following SCI was evaluated using the Basso mouse scale (BMS) scoring<sup>32</sup> (Fig. 1b), footfall tests (Fig. 1c; Supplementary Movie 1), footprint analysis (Supplementary Fig. S2a,b) and electromyography (Supplementary Fig. S2c); T1KO mice recovered from SCI more quickly and more completely than did T2KO, ChABC-treated WT or untreated WT mice (Fig. 1b,c; also see Supplementary Fig. S2d,e). The areas encompassing serotonin-positive (5HT(+)) terminals<sup>1</sup> beyond the lesion site were much larger in T1KO than in untreated WT or ChABC-treated WT mice (Fig. 1d, Table 1 and Supplementary Fig. S2f,g), and there were many more 5HT(+) terminals in T1KO mice (Table 1; see also Supplementary Fig. S2f,g). These observations indicated that functional recovery after SCI was associated with axon regrowth and/or sprouting (Fig. 1d and Table 1) in T1KO mice. Importantly, these effects in T1KO mice were superior to those following ChABC treatment (Table 1 and Supplementary Fig. S2g), and T2KO mice did not show any significant increase in 5HT(+) staining (Fig. 1e and Supplementary Fig. S2f,g). To determine whether the corticospinal tract (CST; a representative pathway operating voluntary movement) recovered, we traced the biotinylated dextran amine (BDA) (+)-extending axons in each group of mice after SCI. Axons that had migrated past a scar

(Supplementary Fig. S3a,b) and into caudal regions were evident only in T1KO SCI mice (Supplementary Fig. S3b). GAP-43 immunoreactivity—which is a marker of neuron growth, growth cones and extending axons<sup>14,33</sup>—was evident in CST axons in caudal regions only in T1KO SCI mice, but not in ChABC-treated WT or T2KO SCI mice (Supplementary Fig. S3c). Following SCI, caudal GAP-43(+)-CST axon terminals were significantly more abundant in T1KO SCI mice than in WT or T2KO mice (Supplementary Fig. S3d,e).

Next, we examined whether the superior recovery and axon regrowth in T1KO animals depended on reduction of CS. We used immunohistochemistry to confirm that ChABC treatment broke CS down (Supplementary Fig. S4a). T1 was highly expressed in some reactive astrocytes in WT mice following SCI, but it was not evident in T1KO mice (Supplementary Fig. S4b). Moreover, CS production in areas with glial scars, which are produced by reactive astrocytes<sup>3</sup>, was much lower in T1KO mice than WT or T2KO mice (Fig. 2a). We also demonstrated biochemically (Fig. 2b) and using morphometrical measurements (Fig. 2c) that CS levels in injured spinal cords of T1KO mice were lower than in those of WT or T2KO mice (Supplementary Fig. S4c). Undoubtedly, several other enzymes are involved in CS synthesis<sup>28</sup> (cf. Fig. 1a), and CS is not completely absent from T1KO mice<sup>29</sup> (Fig. 2c; Supplementary Fig. S4d). Notably, *Caenorhabditis elegans* lacks T1 and T2, yet a chondroitin backbone comprising GalNAc and GlcA is synthesized in worms by four other enzymes (ChSy1–3 and Chpf2) that are also found in mammals<sup>34</sup> (see Fig. 1a); therefore, these four enzymes may synthesize CS in mammals lacking T1, although probably at a much slower rate than when T1 is present.

**Table 1 | Quantification of areas encompassing 5HT(+) terminals.**

	2~3 mm rostral	Lesion	2~3 mm caudal	4~5 mm caudal
WT	8,780 ± 1,345	926 ± 21	85 ± 10	30 ± 11
T1KO	8,942 ± 1,137	365 ± 32	2,779 ± 897*	2,025 ± 910*
T2KO	8,765 ± 1,029	902 ± 41	72 ± 12	26 ± 13
ChABC	6,238 ± 3,547	643 ± 92	779 ± 615*	1,151 ± 505*

ChABC, ChABC-treated; Sham, Sham-operated.

The areas encompassing 5HT(+) terminals in the ventral horn were measured 6 weeks after injury<sup>32</sup> (see also Supplementary Fig. S2e). Data are expressed as the mean ± s.e.m. ANOVA and Bonferroni's multiple comparison test (Prism 5.04); *n* = 9;

\**P* < 0.05 (versus WT).

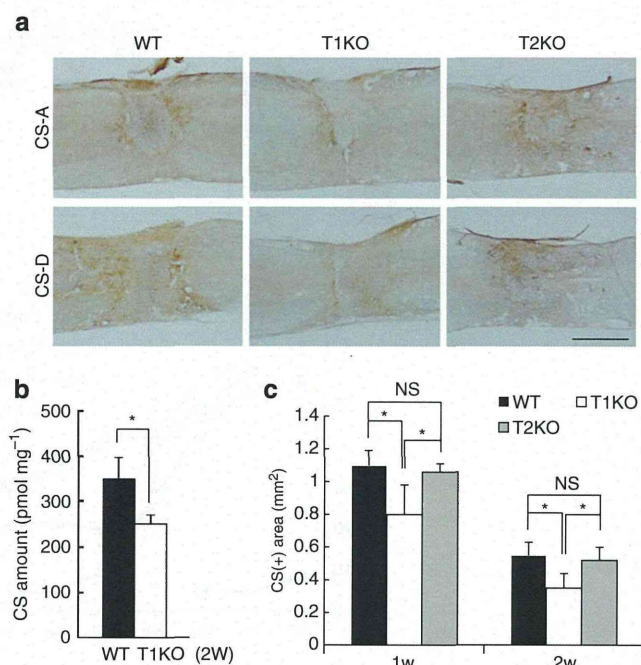


**Figure 2 | CS synthesis after the CSI is lower in T1KO than in WT mice.**

(a) Following SCI, CS expression 2 weeks after the injury was considerably lower in T1KO mice than in WT or T2KO mice. Anti-CS-A and anti-CS-D antibodies recognize two distinct sugar chain units of CS. Scale bar, 1 mm. (b) CS accumulation following SCI was lower in T1KO than in WT mice. \**P* < 0.05 (Student's *t*-test; *n* = 5). (c) CS(+) areas were smaller in T1KO (grey) mice than in WT (white) or T2KO (grey) mice. Repeated-measures ANOVA followed by the Bonferroni-Dunn test. \**P* < 0.05 (*n* = 6). Data are expressed as the mean ± s.e.m. in **b** and **c**.



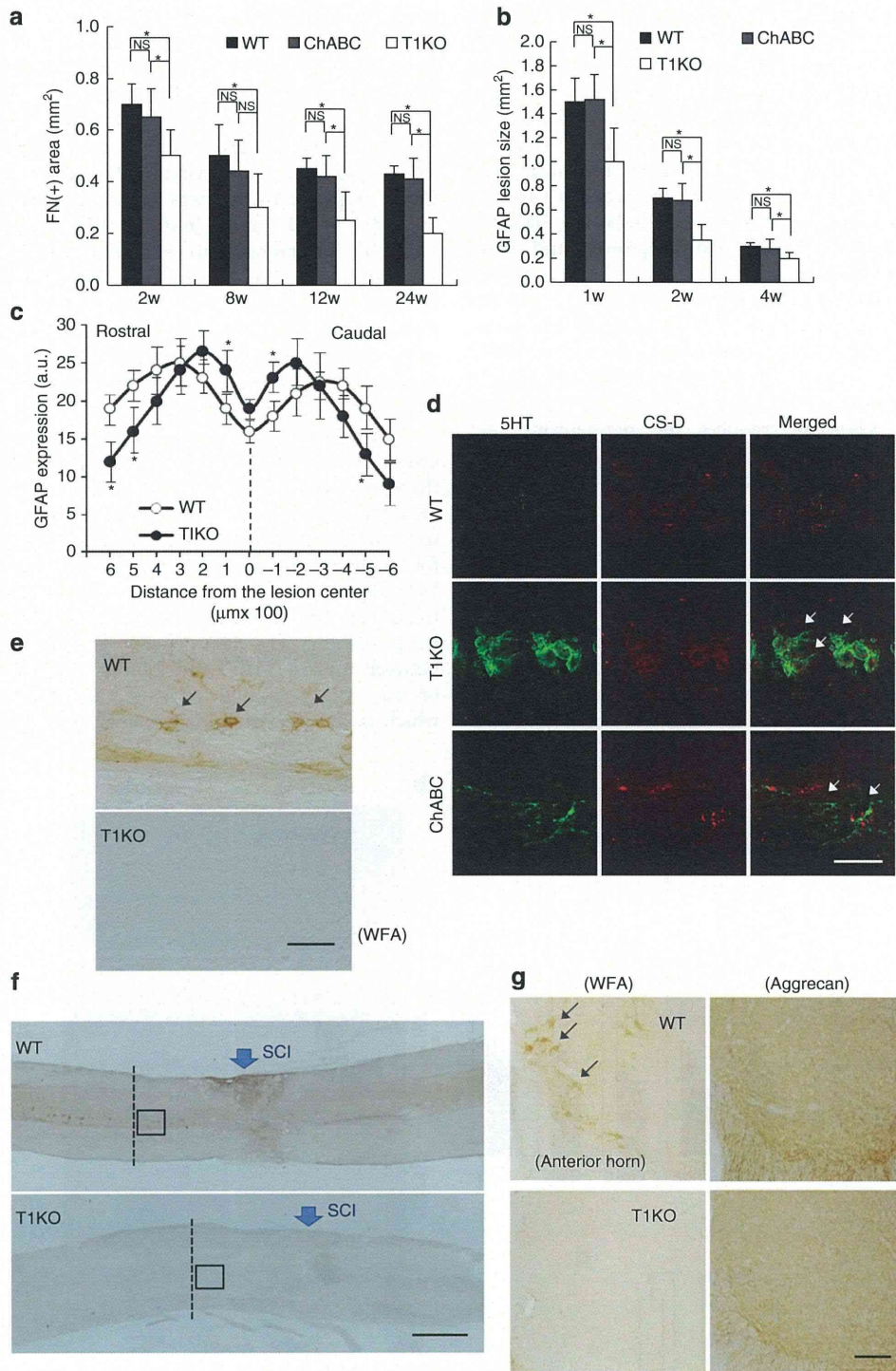


**Figure 3 | Reduced CS levels are associated with reduced scar formation in T1KO mice.** In **a** and **b**,  $n = 7$ ; and in **c**,  $n = 5$ . (**a,b**) Fibrotic scar areas (**a**) and glial scar areas (**b**) were smaller in T1KO mice (grey) than in WT (white) or in ChABC-treated mice (ChABC; black). Data are expressed as the mean  $\pm$  s.e.m. These data were compared by two-way ANOVA and Bonferroni's *post hoc* pairwise comparisons;  $*P < 0.05$ . (**c**) Glial scars in T1KO mice covered a narrow area that surrounded the lesion centre; these areas were narrower than those in WT mice (2 weeks after SCI). Data are expressed as the mean  $\pm$  s.e.m. Scheffe's *post hoc* tests at each spinal segment showed significant differences between T1KO and WT mice at  $-5$ ,  $-1$  (caudal) and  $1$ ,  $5$ ,  $6$  (rostral) mm away from the lesion epicentre ( $*P < 0.05$ ). (**d**) Distribution of 5HT(+) terminals after recovery from SCI in T1KO mice was different from that in ChABC-treated (ChABC) mice. Many sprouting 5HT(+) terminals had accumulated in extracellular matrix around the cells in T1KO, but not in ChABC-treated mice. Arrows indicate the regrowing 5HT(+) terminals. Scale bar,  $50 \mu\text{m}$ . (**e-g**) PNNs after SCI were not evident in T1KO mice. Higher (**e**) and lower (**f**) magnifications of WFA-labelled PNNs in WT and in T1KO 3 weeks after SCI. PNNs were evident in WT but not in T1KO mice. The boxed areas in **f** are magnified in **e**. Scale bars,  $1 \text{ mm}$  (**e,f**). (**g**) Coronal sections of the anterior horn were taken along the axis represented by the dotted line in **f** and stained via WFA or with anti-aggrecan antibody (aggrecan). In T1KO mice, WFA-labelled CS concentrated in PNN was not evident but signal from aggrecan, a core CSPG protein, was evident. Scale bars,  $50 \mu\text{m}$ .



Nevertheless, fibrotic scars (Fig. 3a) and glial scars<sup>3,19–20</sup> (Fig. 3b) were much smaller in T1KO mice than in WT or ChABC-treated mice (Fig. 3a,b; Supplementary Fig S3a). In contrast, scar area did not differ significantly between ChABC-treated and WT mice (Fig. 3a,b). Each glial scar in T1KO mice was limited to a narrow area that surrounded the centre of the SCI lesion (Fig. 3c; Supplementary Fig. S3a). 5HT(+) terminals in T1KO mice were highly concentrated around the astrocytes but scars in ChABC-treated mice were not (Fig. 3d). These results indicated that both effects of T1KO—more complete axon regrowth and more regrowing axon terminals (Fig. 1b–d, and Table 1)—were related to a reduction in the ‘barrier’ scar area and that this reduction was a result of decreased CS production<sup>3,6,7</sup> (Figs 2 and 3). Moreover, each effect was probably independent of residual CS in T1KO mice because ChABC treatment caused more CS degradation and led to worse outcomes than did T1KO (Fig. 3a,b and Table 1). ChABC treatment reportedly reduces the perineuronal net (PNN), which is enriched with CS and inhibits neural plasticity<sup>35</sup>; moreover, reductions in the PNN reportedly enhance neuronal plasticity, neuronal sprouting and recovery from SCI<sup>36,37</sup>. Therefore, we examined the PNN in mice recovering from induced SCI. We used *Wisteria floribunda* agglutinin (WFA), a generalized marker of PNN, to assess PNNs and found that WFA was evident in WT mice but not in T1KO mice (Fig. 3e–g).

#### Increased HS synthesis in T1KO mice promotes rapid recovery.

On the basis of histological and phenotypic features of T1KO

mice, we doubted that the 25% reduction in CS (Fig. 2c) in T1KO mice was solely responsible for such complete recovery from SCI (Fig. 1b–d, Table 1 and Supplementary Fig. S2a,b,d,e,g). Therefore, we suspected that changes in HS synthesis might also be involved because T1 and some HS-synthesis enzymes share the tetrasaccharide linker as a substrate<sup>24,28</sup> (Fig. 1a). The expression of enzymes other than T1 that synthesize CS in response to SCI was not significantly different between injured T1KO and injured WT mice (Supplementary Fig. S5a). Surprisingly, however, the expression of HS-synthesis enzymes—including Ext1 and Ext2, which are essential to HS synthesis (Fig. 1a)—was much higher in injured T1KO mice than that in uninjured T1KO or injured WT mice (Fig. 4a). Importantly, ChABC treatment did not cause upregulation of these HS-synthesis enzymes (Supplementary Fig. S6a).

On the basis of these results, we strongly suspected that HS synthesis contributed to the superior recovery of T1KO mice; therefore, we examined HS expression after SCI. HS-positive areas were significantly larger in the injured spinal cords of T1KO mice than in those of WT mice (Fig. 4b), and HS levels were 20-fold higher in the injured regions of T1KO mice than in those of WT (Fig. 4c; Supplementary Fig. S6b). Notably, neither ChABC treatment nor T2 knockout increased HS levels (Fig. 4b,d; Supplementary Fig. S6c). There were no significant differences between injured T1KO and injured WT mice in the expression of any CS-containing proteoglycan (CSPG) or syndecan-3, which is an HS-containing proteoglycan (HSPG; Supplementary

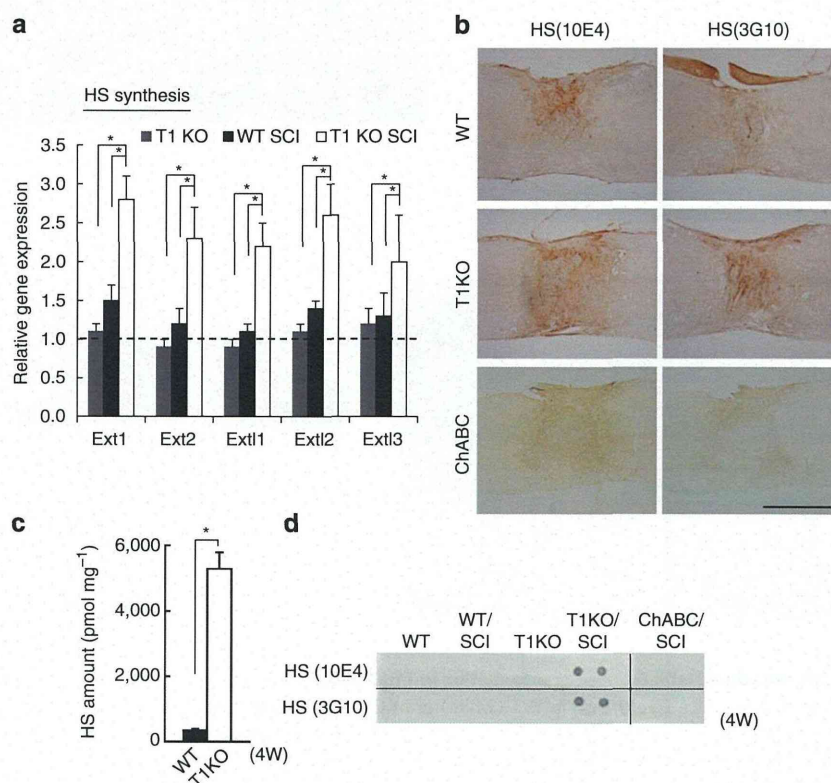


**Figure 4 | HS synthesis increases in injured spinal cords of T1KO mice.** T1KO, T1-null; WT, wild type. Data are expressed as the mean  $\pm$  s.e.m. (a,c). (a) Expression of messenger RNAs encoding enzymes necessary for HS synthesis was assayed via reverse transcriptase-PCR. The level of mRNA expression in WT mice was defined as 1.0 for each gene. These data were compared by two-way ANOVA and Bonferroni's *post hoc* pairwise comparisons.  $*P < 0.05$  ( $n = 15$ ); T1KO SCI versus WT SCI or versus T1KO (intact). (b) On the basis of immunohistochemistry, HS was highly expressed in T1KO mice but not in WT or ChABC-treated mice, 2 w after SCI. Antibodies 10E4 and 3G10 recognize different disaccharides in HS. Scale bar, 1 mm. (c) Biochemical quantification of HS expression at sites of SCI 2 weeks after injury.  $*P < 0.05$  (Student's *t*-test;  $n = 6$ ). (d) Dot-blot analysis of HS expression in spinal cords before and after SCI (2 w). HS was detected only in T1KO mice with SCI, but not in any other mice, including the ChABC-treated mice.



Fig. S6a,d). To assess whether this upregulation of HS synthesis in T1KO mice following SCI promoted axon regrowth or sprouting, we examined the effects of continuously administered bacterial heparitinase (HSase), which degrades HS<sup>30</sup>, on recovery from SCI. On the basis of BMS scoring (Fig. 5a) and footfall tests (Fig. 5b), HSase treatment slowed the recovery of T1KO mice (Fig. 5 and Table 2), as did RNA interference (RNAi)-mediated knockdown (KD) of an HS-synthesis enzyme, Ext1 (Fig. 5 and Table 2). In addition, HSase treatment reduced the area encompassing regenerating 5HT(+) axon terminals in T1KO mice to a level similar to that in WT mice (Table 2), but the recovery in ChABC-treated mice was not sensitive to HSase, suggesting that ChABC did not induce HS upregulation (Supplementary Fig. S6a,e). These results indicated that upregulation of HS synthesis in T1KO mice promoted axon regrowth and/or sprouting and functional recovery from SCI, just as it promotes axon growth during CNS development<sup>5,25</sup>.

We tried to identify the target HSPGs in injured T1KO mice that bore the upregulated HSase-sensitive HS. HS-modified syndecan-3 (*N*-syndecan) and glypican-1 were highly expressed (Fig. 6a and Supplementary Fig. S6d) and widely distributed (Fig. 6b) at sites of SCI in T1KO mice. In the injured spinal cords of T1KO mice, both HSPGs were detected via HS-specific antibodies (Fig. 6c) and had HSase-sensitive HS chains (Fig. 6d); importantly, in WT SCI mice, degraded HS derived from these two HSPGs was barely evident, indicating that the upregulated HSase-sensitive HS was specifically bound to syndecan-3 and glypican-1 in injured T1KO (Fig. 6d).

After SCI, Ext2 was expressed in neurons<sup>30</sup> of T1KO mice (Fig. 7a), and the expression of HS-synthesis enzymes was upregulated in neuron-rich areas rather than in areas of glial scarring (Fig. 7b); therefore, we concluded that extra HS was produced by the neurons<sup>5,24,25</sup> that expressed HS-synthesis enzymes such as Ext2. Receptor protein tyrosine phosphatase- $\sigma$  (RPTP $\sigma$ ), a receptor for both HSPGs and CSPGs<sup>38,39</sup>, was also upregulated in T1KO mice after SCI, and RPTP $\sigma$  co-localized with some of the regrowing and/or sprouting axons (Supplementary Fig. S7a-d). HS, unlike CS, is known to promote axon growth during neural development<sup>5,24,25,31,39</sup>; therefore, our data indicated that GAG synthesis in T1KO mice was more favourable to axon regrowth than was the GAG

synthesis in WT mice. To assess whether upregulation of HS was directly involved in neurite growth following SCI and whether effects of RPTP $\sigma$  on neurite growth depended on HS, we examined the effects of concurrent overexpression of Ext1 and Ext2 on cultured neurons (Fig. 7c). Ext1-Ext2 overexpression induced neurite growth in an HSase-sensitive (Fig. 7c) and RPTP $\sigma$ -sensitive (Supplementary Fig. S7e) manner<sup>39</sup>, indicating that upregulation of HS contributed to axon growth. Therefore, HS-synthesis enzymes such as Ext2 may promote axon growth intrinsically in neurons by targeting new HS synthesis to syndecan-3, glypican-1 or both<sup>40</sup>. RPTP $\sigma$  messenger RNA expression and RPTP $\sigma$  levels were elevated in WT, ChABC-treated and T1KO mice (Supplementary Fig. S7c,d), indicating that at least the increased axon regrowth was not due to a RPTP $\sigma$ -dependent reduction in CS.

RNAi-mediated T1 KD (T1-KD) *in vivo* led to excellent recovery from SCI (Supplementary Fig. S8a-e). T1-KD-associated scars were similar in size to T1KO-associated scars (Supplementary Fig. S8f). T1-KD caused reduced CS synthesis (Supplementary Fig. S8g), and scar sizes were significantly smaller following T1-KD than following ChABC treatment (Supplementary Fig. S8h). Moreover, downregulation of CS synthesis and upregulation of HS-synthesis enzymes were induced by simultaneous T1-KD and T2-KD, as well as by T1KO (Supplementary Fig. S9a-c and Fig. 4, also see

**Table 2 | Quantitative analysis of the area of the caudal region covered by 5HT(+) terminals after HSase treatment 4 weeks after injury.**

	2~3 mm rostral	Lesion	2~3 mm caudal	4~5 mm caudal
WT + PBS	8,501 ± 1,522	799 ± 31	81 ± 11	32 ± 14
T1KO + PBS	8,862 ± 1,204	415 ± 51	2,398 ± 991*	2,012 ± 813*
T1KO + HSase	5,703 ± 3,134	512 ± 107	719 ± 337*	698 ± 173*
ChABC + HSase	6,021 ± 3,467	740 ± 153	800 ± 593*	1,003 ± 566*

ChABC, ChABC-treated; HSase, HSase-treated.

These data were compared by two-way ANOVA and Bonferroni's multiple comparison test (Prism 5.04). T1KO + PBS versus T1KO + HSase, WT + PBS or ChABC + HSase.

\* $P < 0.05$  ( $n = 5$ )

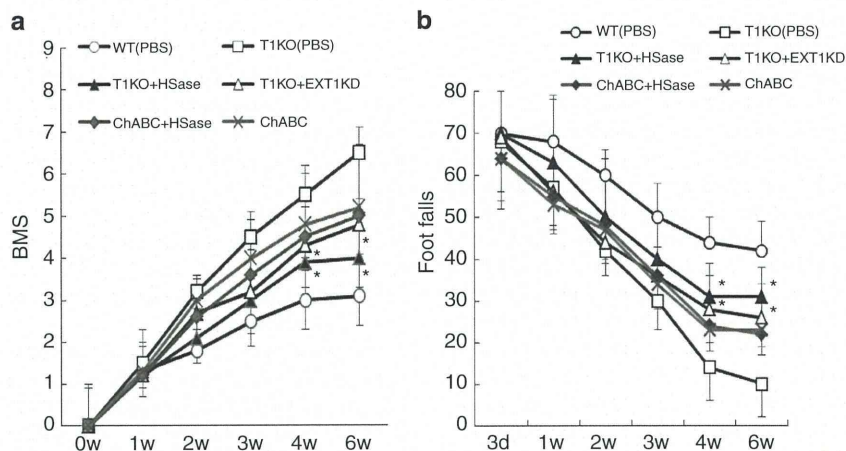


**Figure 5 | Increased HS promotes more rapid and more complete recovery from SCI.** T1KO, T1-null; WT, wild type. Data are expressed as the mean  $\pm$  s.e.m. (a) BMS scores and (b) footfall tests with or without reduction of HS in WT, T1KO and ChABC-treated mice; ChABC was used at 0.2 U per 00  $\mu$ l. HSase (0.4 U per 200  $\mu$ l; experimental treatment) or PBS (control treatment) was administered via a minipump. *EXT1KD*; KD of Ext1 by *in vivo* RNAi (100 nmol per 200  $\mu$ l); also see Supplementary Fig. S8a. *Post hoc* analyses were conducted using the Bonferroni-Dunn test for repeated-measures ANOVA. \* $P < 0.05$  ( $n = 5$ ; in a and b). The BMS subscore for T1KO versus T1KO + HSase mice or versus T1KO + EXT1KD were significantly different at 4 and 6 weeks after SCI.



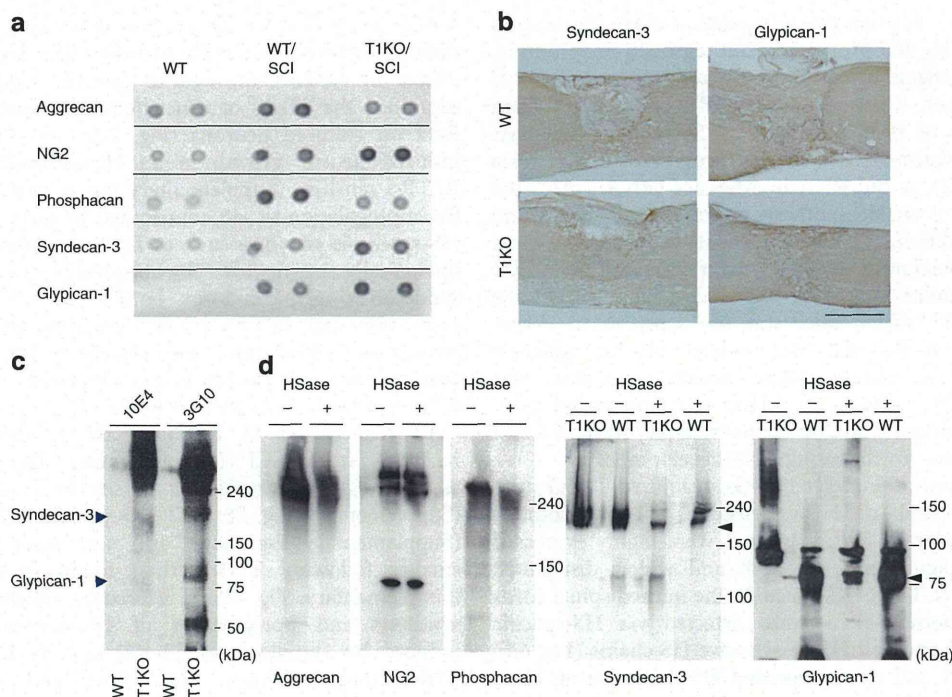


**Figure 6 | Syndecan-3 and glypican-1 are the target HSPGs of SCI-induced HS upregulation in T1KO mice.** (a,b) Syndecan-3 and glypican-1, HSPGs derived from neurons, were expressed in T1KO mice after SCI (2 weeks). (a) Dot-blot analysis of the major core proteins decorated with CSPG or HSPG. (b) Immunohistochemistry of syndecan-3 and glypican-1 after SCI (2 weeks) in WT and in T1KO mice. Scale bar, 1 mm. (c) HSase-treated HSPGs detected by 3G10, the antibody that recognized the HS stub. At least three distinct HSPGs were recognized by 3G10 in T1KO SCI mice, but not in WT SCI mice, including 180 kDa (syndecan-3) and 65–80 kDa (glypican-1). (d) Western-blot analysis of PGs near the lesion sites before (–) and after (+) HSase treatment (5 mU; 37 °C, 3 h). Notably, syndecan-3 and glypican-1 were the main PGs with HSase-sensitive HS in injured T1KO mice. The data for CSPG core proteins (aggrecan, NG2 or phosphacan) are shown only for the injured T1KO mice, and each CSPG was HSase insensitive. Arrows indicate the position of deglycosylated proteins. Numbers on the right indicate molecular masses (kDa).

Supplementary Fig. S5a,b); notably, T1-KD alone was insufficient to cause both effects (Supplementary Fig. S9c,d; compared with Supplementary Fig. S9a,b).

## Discussion

T1KO mice had significantly better recovery from SCI than did WT or ChABC-treated mice (Fig. 1b–d); three distinct phenomena were responsible for this superior recovery. First, T1KO reduced CS synthesis and resulted in smaller scars than did ChABC treatment; reduced scarring probably contributed to better recovery because the smaller scars introduced smaller physical and weaker chemical barriers to the regrowing or the sprouting axons (Figs 1e, 2c and 3a–d, and Supplementary Fig. S2f). In addition, T1KO probably reduced CS concentrations (Fig. 3e). Notably, reduction of CS was apparently superior to complete elimination of CS for SCI recovery, probably because CS has some positive roles in recovery (Fig. 8a). Second, simultaneous upregulation of HS synthesis and downregulation of CS in T1KO mice were essential to excellent recovery from SCI. HS promotes axon growth<sup>5,24,25</sup>, and syndecan-3, a target HSPG of SCI-induced HS upregulation, is enriched in axons and the extracellular matrix around axons<sup>41</sup>. T1KO and T1-KD + T2-KD (Supplementary Fig. S9c) produced the most favourable environment for recovery from SCI; specifically, these treatments shifted conditions at the injury away from the non-permissive CS-rich state (Fig. 8a,b). It is evident that T1KO was substantially superior to ChABC treatment specifically because HS synthesis was stimulated by T1KO and never by ChABC treatment (Fig. 5a,b, Table 2 and Supplementary Fig. S5a,d). HSPGs are important for signal transduction, axon

growth and axon guidance<sup>24,42</sup>; therefore, our findings are very important to axon regeneration. Third, expression of HS chains on both syndecan-3 and glypican-1 and expression of HS-synthesis enzymes (for example, Ext2, Ext1 and Extl2) in neurons were essential to the superior recovery from SCI of T1KO mice (Figs 4a,d, 6a,c and 7a,b). Taken together, our results and those from two previous reports indicated that Ext2 satisfies the definition of a potential intrinsic growth regulator in neurons; the most relevant findings are that Ext1/2 expression is developmentally downregulated in the CNS<sup>43</sup> and that Ext2 and syndecan-1 expressions in neurons are specifically upregulated during peripheral nerve regeneration<sup>30</sup>. Lack of T1 evidently induced these intrinsic positive regulators of axon growth<sup>4,10</sup>. These HS-synthesis enzymes belong to a newly identified group of ‘development-dependent factors with axon growth-promoting features’ and are totally different from previously described factors such as PTEN and KLFs<sup>9,11</sup>. Therefore, we conclude that T1KO and ChABC treatment led to recovery from SCI by very distinct mechanisms.

The following two strategies for controlling CS synthesis have been developed: first, a deoxyribozyme targeting *Xylt1* (see Fig. 1a) messenger RNA inhibits synthesis of the first residue of the tetrasaccharide linker<sup>44,45</sup>. Second, genetic ablation of Sox9, a transcription factor, inhibits expression of some CS-synthesizing enzymes (for example, *Xylt1/2* and *C4st1*)<sup>46</sup>. Each strategy is effective in inhibiting CS synthesis and in improving recovery from SCI. However, based on our new findings, inhibition of T1 should be better than either of those strategies because both of those strategies should inhibit HS synthesis, and HS synthesis promotes axon growth.



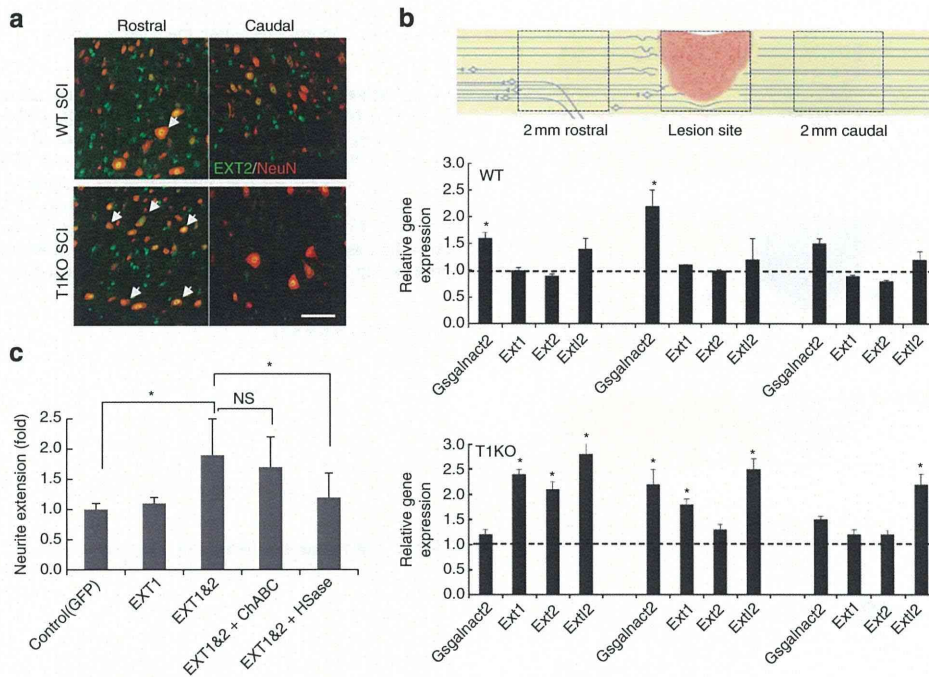


**Figure 7 | Elevated expression of HS is necessary to axon regrowth.** WT/SCI, WT after SCI; KO/SCI, T1KO after SCI. **(a)** Ext2 (green), an essential enzyme for HS sugar chain synthesis, was upregulated in and localized to neurons of T1KO mice after SCI. NeuN (red), a neuronal marker; Ext2-expressing cells (arrows). Scale bars, 20  $\mu$ m. **(b)** Reverse transcriptase (RT)-PCR of genes encoding enzymes involved in GAG synthesis after SCI. The samples were collected from three sites in wild-type (WT) or T1KO mice: 2 mm rostral from the lesion centre (left), the lesion centre (centre) and 2 mm caudal from the lesion centre (right). The samples were analysed using RT-PCR. Notably, the rostral site was mainly composed of neurons, not of reactive astrocytes (the left-most cartoon). The average expression of each gene in intact WT or in intact T1KO mice was defined as 1.0. Expression of each gene (*Csgalnact2* (*T2*), *Ext1*, *Ext2* or *Extl2*) in T1KO versus that in WT. \* $P < 0.05$  ( $n = 6$ ; Bonferroni's comparison test). **(c)** Overexpression of *Ext1*/*Ext2* promoted axon outgrowth of WT cortical neurons in an HSase-dependent manner. Both *Ext1* and *Ext2* complementary DNAs (*Ext1* and 2) were transfected into cultured neurons. The *Ext1* and *Ext2* proteins are thought to form a heterodimeric complex during HS synthesis; overexpression of *Ext1* alone did not result in a significant change. \* $P < 0.05$  (one-way ANOVA;  $n = 4$ ); *Ext1&2* versus control (*GFP*) or versus *Ext1&2* + HSase. In each individual experiment, 100 neurons were counted and the experiments were performed at least three times. Data are expressed as the mean  $\pm$  s.e.m. in **b** and **c**.

In conclusion, our results demonstrate that knocking out a single enzyme, T1, caused both reduced CS synthesis and increased HS synthesis and that manipulation of this single enzyme resulted in the reduction of extracellular inhibitors and the induction of intrinsic growth promoters of axon regeneration. Therefore, our findings provide a novel principle for development of axon regeneration strategies. Chemicals that specifically inhibit T1 might be effective treatments for SCI; however, we need to know the molecular mechanisms by which neuronal HS-synthesis genes (for example, *Ext2*) were upregulated in T1KO mice. Finally, adding inhibition of TI to other treatments<sup>36,47</sup> for SCI may improve overall clinical outcomes.

## Methods

**Materials.** ChABC and HSase (HSase I/III), heparanase I and II, WFA and Ate-loGene Local Use Kits for atelocollagen-mediated *in vivo* short interfering RNA were purchased from Seikagaku Corp. (Tokyo, Japan), from IBEX Technology Inc. (Montreal, Canada), Vector Laboratories Inc. (Burlingame, CA, USA) and from KOKEN Co. Ltd. (Tokyo, Japan), respectively. An osmotic minipump (Model 2006 (for 7W long) and Model 2004 (for 4W long)), catheter tubing (Mit-02) and the infusion kit were purchased from ALZET (Cupertino, CA). Antibodies used in this study are listed in Supplementary Table S1 (As for the two antibodies provided from other researchers, listed in this Table, please refer to refs 48,49).

**Generation of T2KO.** All animal experimental studies were conducted with the approval of the Animal Care and Use Committee of Niigata University. T1KO<sup>29</sup> mice were derived from the C57BL/6N strain. For most experiments, the WT strain used was C57BL/6N; the ICR strain was used only for the *in vivo* RNAi studies. T2KO mice were generated via the methods used to generate T1KO mice<sup>31</sup>. The

mouse *T2* gene was identified as NM\_030165. Exon 5 of mouse *T2* encodes a DXD motif, which is a binding site for  $Mn^{2+}$  that is essential to the *in vitro* activity of most GalNAc/Gal transferases<sup>50</sup>; therefore, we designed a targeting vector with the mouse *T2* exon 5 located between two loxP sites (Supplementary Fig. S1a). The T2KO mice were generated using an embryonic stem (ES) cell line derived from C57BL/6N mice; this line is designated RENKA. Resulting chimeric mice were mated to C57BL/6N mice and heterozygous offspring (*C5GalNAc2*<sup>+/flox(neo)</sup>) were mated to *telencephalin-cre* mice<sup>29</sup>.

**Induction of SCI.** Mice (8–10 weeks old, C57BL/6J, male) were subject to compression-induced SCI; a bilateral contusion injury was induced at the 10th thoracic vertebrae (Th10) of individual mice with a commercially available SCI device (Infinite Horizon Impactor; Precision Systems and Instrumentation, Lexington, NY)<sup>20,32</sup>, except that here we used a 70-kdyne impact force. The device reports data regarding time versus force and time versus displacement. The locomotor recovery assessment was performed using video recording<sup>32</sup>, and BMS open-field scoring was used to test mice once weekly for functional recovery during the 6–8 weeks following SCI<sup>32</sup>. The evaluations were scored independently by two investigators who were unaware of the experimental groups (at least eight mice in each group). On the third day after induction of SCI, mice were excluded if they had an incomplete injury (BMS score > 0 on that day). Morphometric assays were performed using SCI samples prepared from the sagittal sections at 12  $\mu$ m intervals<sup>32</sup>.

For each footfall test, a mouse was placed on a wire mesh grid and videotaped for 5 min while on the grid. To be scored, an animal had to walk for a minimum of 3 of the 5 min as determined by three independent examiners; for each animal scored, the total number of the footfalls from the bars was counted, and the total walking time was recorded.

To assess stepping patterns of hind limbs during forward locomotion after injury, the bottom of a well-lit runway (3 cm wide and 100 cm long) was lined with white paper, and mice were required to run along the runway in a darkened box. To record footprints, the planter surfaces of hind limbs were brushed with ink during continuous locomotion across a paper.



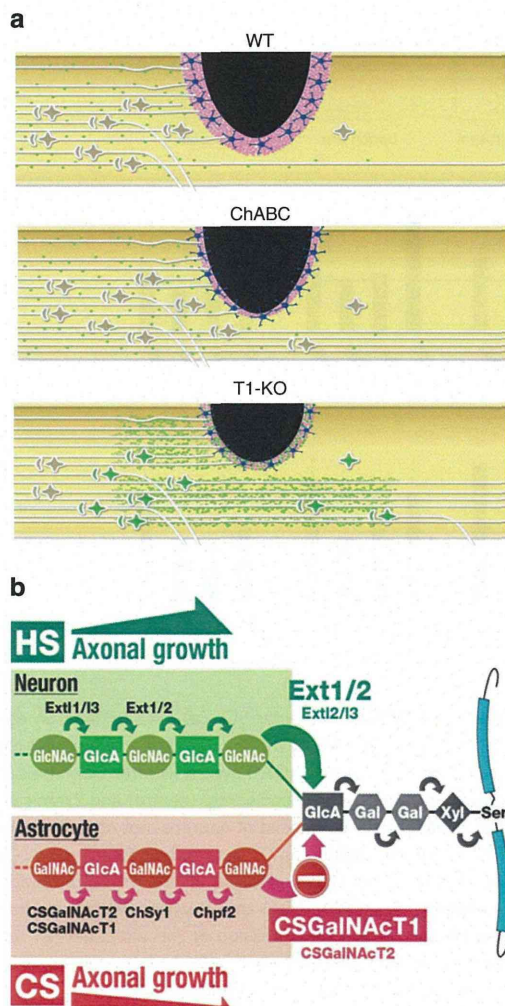


**Figure 8 | Schematic model of T1-regulated GAG balance after SCI.**

(a) Summary of the results on SCI recovery. In WT (uppermost) mice, CS (dark pink) production was elevated in the reactive astrocytes (star-like form in blue), and thick scars (black)<sup>3</sup>, which inhibited axon regeneration, formed; consequently, very few regenerating axons could migrate to areas past the SCI lesion. In contrast, in T1KO mice (middle), CS production was reduced and the scars were smaller than those in WT mice. In addition, HS (green) expression was high in T1KO neurons, and the number of regrowing or sprouting axons was higher than that in WT. Although ChABC-treated mice (ChABC; lowermost) had less CS than did WT or T1KO, they had larger scars than T1KO mice, and they did not overproduce HS; therefore, axonal regeneration was reduced and restricted relative to that in T1KO. WT and ChABC-treated mice, unlike T1KO mice, experienced only baseline levels of HS synthesis after SCI; these baseline levels could not promote recovery from SCI. (b) Possible biochemical mechanism that promotes better recovery from SCI in T1KO mice<sup>26</sup>. In WT, T1 is upregulated in reactive astrocytes after SCI; however, *Ext1* and *Ext2*, which are genes with putative 'axon growth-promoting activity/potential', are upregulated in neurons of T1KO mice, and T1 is not expressed (minus in red); consequently, HS, rather than CS, accumulates around T1KO neurons. As a result, the amount of CS decreases and that of HS increases, and this shift in the CS-HS balance promotes axon regrowth<sup>39</sup>. As increases in HS and decreases in CS persist, the potential for axon growth is elevated.

The electrophysiological experiments to evaluate motor function resulting from evoked potential of the neuromuscular function were performed by short trains of five square-wave stimuli of 0.5 ms duration with an interstimulus interval of 3 ms (ref. 32). The active and the reference electrodes were placed in the muscle belly, and near the distal tendon of the muscle in each limb<sup>32</sup>, respectively. Scorps3

software (AD Instruments, New South Wales, Australia) was used to average and analyse 100 responses including the latency period.

**Quantitative real-time PCR.** Total RNA was extracted from the SCI regions using an RNeasy FFPE kit or an ALL prep RNA kit (QIAGEN). Total RNA (0.5 µg) was used as template; the iScript one-step RT-PCR kit (Bio-Rad), the SsoFast Probes supermix (Bio-Rad) and the PrimeTime qPCR assay (Integrated DNA Technologies, IW) were used for real-time reverse transcriptase-PCR; the reaction parameters were as follows: 95 °C for 30 s; and 40 cycles at 95 °C for 2 s and 65 °C for 5 s; 65–95 °C for 2 s) as indicated in the Taqman probe (Life Technologies) gene expression assay materials. Nucleotide sequence of real-time quantitative PCR primers and ZEN double-quenched probes are listed in Supplementary Table S2.

**In vivo RNAi after SCI.** For the *in vivo* RNAi studies, SCI was induced in ICR mice (8–10 w; Clea Japan, Inc.) with the IH impactor as described above except that the impact force was 100 kdynes. Just after the SCI contusion, gelfoam impregnated with a mixture containing one or two siRNAs (10 µM each) and AtoGen Local Use Kit (see Materials) was placed on the lesion area<sup>51–53</sup>. RNA sequences of the siRNAs used in these experiments are listed in Supplementary Table S3<sup>34</sup>. The scrambled sequences of the negative-control siRNAs had four or five nucleotides that differed from the corresponding nucleotides in the targeted siRNAs.

**ChABC and HSase treatments in vivo.** Continuous ChABC treatment after SCI was performed using an osmotic pump<sup>14,55</sup> set at the 10th thoracic vertebrae levels for up to 2 weeks (200 U ml<sup>-1</sup> in a volume of 0.2 ml). For the HSase application, an osmotic minipump (ALZET, Cupertino, CA; Model 2006) was implanted subcutaneously and used to infuse HSase (0.2 unit per 6 µg) dissolved in saline containing 0.05% BSA or vehicle into the contusion site through a flexible plastic cannula because HSase is less stable than ChABC *in vivo*.

**Immunohistochemistry.** The dilution ratios for each antibody are listed in Supplementary Table S1. Tissue sections were incubated with biotinylated secondary antibody and then with avidin-biotin peroxidase complex<sup>55,56</sup> (Vectastain ABC kit; Vector Laboratories Inc.). Digital images were taken with a confocal laser scanning microscope (Zeiss, LSM5 exciter) and AxioVision charge-coupled device camera (Carl Zeiss). Spinal cord cryosections (20 µm thick) were obtained from mice that had been transcardially perfused with 4% formaldehyde. Standardized areas for sampling<sup>32</sup> in the central regions (10 sections) were calculated using Image J (NIH) and MetaMorph (Molecular Devices). For analysis of 5HT(+) sprouting axons and boutons, rectangular areas were set 1–3 mm distal to the central line of the lesion site in each section<sup>32</sup>, and 10 sagittal sections from each mouse were used for quantitative analysis.

**Anterograde labelling of the CST.** Exactly 8 weeks after injury, BDA (10% in saline, molecular weight 10,000 Da; Molecular probes)<sup>6</sup> was injected into the motor cortices to label the descending CST fibres. The injection site was precisely 2.1 mm posterior to the bregma, 2 mm lateral to the bregma and 0.7 mm deep. We performed pressurized injections with a glass capillary attached to a microsyringe (Narishige) at a rate of 0.1 µl min<sup>-1</sup> until the desired amount was injected. Exactly 2 weeks after each injection, the animals were anaesthetized and perfused with PBS and then with 4% paraformaldehyde in PBS. We used Alexa Fluor 488-conjugated streptavidin (Invitrogen) and the Vectastain ABC Elite kit (Vector Laboratories Inc.) or a tyramide signal amplification fluorescence system (Perkin Elmer) to fluorescently label the BDA.

**Quantification analysis of GAGs from the spinal cord.** GAG analyses were conducted by enzymatic treatment and HPLC-based quantification<sup>29,57</sup>. GAGs were extracted from spinal cord tissue samples by incubating the samples in a protease solution (0.01 mg actinase E, 10 mM CaCl<sub>2</sub>, 50 mM Tris-HCl (pH 8.0)) at 55 °C for 2 days. After addition of trichloroacetate, each extract was centrifuged at 15,000 g for 20 min. Each partially purified CSPG and HSPG fractions were digested with ChABC (5 mIU ChABC in 60 mM CH<sub>3</sub>COONa, 50 mM Tris-HCl (pH 8.0)) or HSase (0.5 mIU HSase in 20 mM CH<sub>3</sub>COONa, 2 mM (CH<sub>3</sub>COO)<sub>2</sub>Ca (pH 7.0)), respectively. GAGs in each digest were derivatized using 2-aminobenzamide; these mixtures were analysed using HPLC (column: YMC pack PA, elution: 16–530 mM NaH<sub>2</sub>PO<sub>4</sub>)<sup>57</sup>.

**Neuronal cell culture.** Cortical neurons were prepared from embryonic day 17 or postnatal day 1 mice<sup>33</sup>, and were then transfected with a human *Ext1* construct in a pCMVvector (Takara Bio Co., Otsu, Japan), a human *Ext2* construct in the pcDNA3.1 vector (Invitrogen) or a combination thereof. Stealth Select RNAi (Invitrogen, s72517, s72516 and s72518) was used to knockdown RPTPσ expression. In some cultures, ChABC (2 mU) or HSase (2 mU) was added 12 h after transfection. Cells were stained with anti-HS 10E4 antibody 48 h after transfection. The sequences of siRNAs targeting RPTPσ are listed in Supplementary Table S3. siRNAs with scrambled sequence (Invitrogen) were used as negative controls.



**Statistics.** Data are presented as mean values  $\pm$  s.e.m. Prism version 5.04 software (GraphPad) or SPSS statistics software (IBM) were used for to perform statistical analyses. Unpaired two-tailed Student's *t*-tests were used for single comparisons. Analysis of variance (ANOVA; one-way, two-way or repeated-measures ANOVA) were used for multiple comparisons; Bonferroni's procedure were used to assess *post hoc* pairwise differences. Repeated-measures ANOVA was used to analyse BMS and footfall scores with follow-up comparison of treatments for each day, by contrast *t*-test and correction for multiple comparisons by the Holm method ( $P=0.05$ ). Each investigator was blinded with regard to genotypes during all procedures performed to collect data for subsequent statistical analysis. For analyses of the morphometric data, all evaluations were performed by ANOVA with *post hoc*-independent pairwise analysis.  $P<0.05$  was considered statistically significant. The specific tests used to analyse data from each set of experiments are indicated in the figure legends.

## References

- Tuszynski, M. H. & Steward, O. Concepts and methods for the study of axonal regeneration in the CNS. *Neuron* **74**, 777–791 (2012).
- Esposito, E. & Cuzzocrea, S. Anti-TNF therapy in the injured spinal cord. *Trends Pharmacol. Sci.* **32**, 107–115 (2011).
- Silver, J. & Miller, J. H. Regeneration beyond the glial scar. *Nat. Rev. Neurosci.* **5**, 146–156 (2004).
- Liu, K., Tedeschi, A., Park, K. & He, Z. Neuronal intrinsic mechanisms of axon regeneration. *Annu. Rev. Neurosci.* **34**, 131–152 (2011).
- Bandtlow, C. E. & Zimmermann, D. R. Proteoglycan in the developing brain: new conceptual insights for old proteins. *Physiol. Rev.* **80**, 1267–1290 (2000).
- Bradbury, E. J. *et al.* Chondroitinase ABC promotes functional recovery after spinal cord injury. *Nature* **416**, 636–640 (2002).
- Carulli, D., Laabs, T., Geller, H. M. & Fawcett, J. W. Chondroitin sulfate proteoglycans in neural development and regeneration. *Curr. Opin. Neurobiol.* **15**, 116–120 (2005).
- Lee, J. K. *et al.* Combined genetic attenuation of myelin and Semaphorin-mediated growth inhibition is insufficient to promote serotonergic axon regeneration. *J. Neurosci.* **30**, 10899–10904 (2010).
- Liu, K. *et al.* PTEN deletion enhances the regenerative ability of adult corticospinal neurons. *Nat. Neurosci.* **13**, 1075–1083 (2010).
- Yang, P. & Yang, Z. Enhancing intrinsic growth capacity promotes adult CNS regeneration. *J. Neurol. Sci.* **312**, 1–6 (2012).
- Moore, D. L. *et al.* KLF family members regulate intrinsic axon regeneration ability. *Science* **326**, 298–301 (2009).
- Jones, L. L., Yamaguchi, Y., Stallcup, W. B. & Tuszynski, M. H. NG2 is a major chondroitin sulfate proteoglycan produced after spinal cord injury and is expressed by macrophages and oligodendrocyte progenitors. *J. Neurosci.* **22**, 2792–2803 (2002).
- Zhao, R. R. *et al.* Lentiviral vectors express chondroitinase ABC in cortical projections and promote sprouting of injured corticospinal axons. *J. Neurosci. Methods* **201**, 228–238 (2011).
- Ikegami, T. *et al.* Chondroitinase ABC combined with neural stem/progenitor cell transplantation enhances graft cell migration and outgrowth of growth-associated protein-43-positive fibers after rat spinal cord injury. *Eur. J. Neurosci.* **22**, 3036–3046 (2005).
- Massey, J. M. *et al.* Increased chondroitin sulfate proteoglycan expression in denervated brainstem targets following spinal cord injury creates a barrier to axonal regeneration overcome by chondroitinase ABC and neurotrophin-3. *Exp. Neurol.* **209**, 426–445 (2008).
- Starkey, M. L., Bartus, K., Barritt, A. W. & Bradbury, E. J. Chondroitinase ABC promotes compensatory sprouting of the intact corticospinal tract and recovery of forelimb function following unilateral pyramidotomy in adult mice. *Eur. J. Neurosci.* **36**, 3665–3678 (2012).
- Bradbury, E. J. & Carter, L. M. Manipulating the glial scar: chondroitinase ABC as a therapy for spinal cord injury. *Brain Res. Bull.* **84**, 306–316 (2011).
- Zhao, R. R. & Fawcett, J. W. Combination treatment with chondroitinase ABC in spinal cord injury-breaking the barrier. *Neurosci. Bull.* **29**, 477–483 (2013).
- Rolls, A., Shechter, R. & Schwartz, M. The bright side of the glial scar in CNS repair. *Nat. Rev. Neurosci.* **10**, 235–241 (2009).
- Okada, S. *et al.* Conditional ablation of Stat3 or Socs3 discloses a dual role for reactive astrocytes after spinal cord injury. *Nat. Med.* **12**, 829–834 (2006).
- Sato, T. *et al.* Differential roles of two *N*-acetylgalactosaminyltransferases, CSGalNAcT-1, and a novel enzyme, CSGalNAcT-2: Initiation and elongation in synthesis of chondroitin sulfate. *J. Biol. Chem.* **278**, 3063–3071 (2003).
- Uyama, T., Kitagawa, H., Tamura, J. & Sugahara, K. Molecular cloning and expression of human chondroitin *N*-acetylgalactosaminyltransferase: the key enzyme for chain initiation and elongation of chondroitin/dermatan sulfate on the protein linkage region tetrasaccharide shared by heparin/heparan sulfate. *J. Biol. Chem.* **277**, 8841–8846 (2002).
- Mizumoto, S., Ikegawa, S. & Sugahara, K. Human genetic disorders caused by mutations in genes encoding biosynthetic enzymes for sulfated glycosaminoglycans. *J. Biol. Chem.* **288**, 10953–10961 (2013).
- Nadanaka, S. & Kitagawa, H. Heparan sulphate biosynthesis and disease. *J. Biochem.* **144**, 7–14 (2008).
- Maeda, N., Ishii, M., Nishimura, K. & Kamimura, K. Functions of chondroitin sulfate and heparan sulfate in the developing brain. *Neurochem. Res.* **36**, 1228–1240 (2011).
- Duchez, S. *et al.* Glycotranscriptome study reveals an enzymatic switch modulating glycosaminoglycan synthesis during B-cell development and activation. *Eur. J. Immunol.* **41**, 3632–3644 (2011).
- Uyama, T. *et al.* Molecular cloning and expression of a second chondroitin *N*-acetylgalactosaminyltransferase involved in the initiation and elongation of chondroitin/dermatan sulfate. *J. Biol. Chem.* **278**, 3072–3078 (2003).
- Gulberti, S. *et al.* Chondroitin sulfate *N*-acetylgalactosaminyltransferase-1 (CSGalNAcT-1) involved in chondroitin sulfate initiation: Impact of sulfation on activity and specificity. *Glycobiology* **22**, 561–571 (2012).
- Watanabe, Y. *et al.* Chondroitin sulfate *N*-acetylgalactosaminyltransferase-1 is required for normal cartilage development. *Biochem. J.* **432**, 47–55 (2010).
- Murakami, K. *et al.* Nerve injury induces the expression of EXT2, a glycosyltransferase required for heparan sulfate synthesis. *Neuroscience* **141**, 1961–1969 (2006).
- Kantor, D. B. *et al.* Semaphorin 5A is a bifunctional axon guidance cue regulated by heparan and chondroitin sulfate proteoglycans. *Neuron* **44**, 961–975 (2004).
- Ito, Z. *et al.* *N*-Acetylglucosamine 6-*O*-sulfotransferase-1-deficient mice show better functional recovery after spinal cord injury. *J. Neurosci.* **30**, 5937–5947 (2010).
- Nozumi, M. *et al.* Identification of functional marker proteins in the mammalian growth cone. *Proc. Natl Acad. Sci. USA* **106**, 17211–17216 (2009).
- Izumikawa, T. *et al.* Nematode chondroitin polymerizing factor showing cell/organ-specific expression is indispensable for chondroitin synthesis and embryonic cell division. *J. Biol. Chem.* **279**, 53755–53761 (2004).
- Wang, D. & Fawcett, J. The perineuronal net and the control of CNS plasticity. *Cell Tissue Res.* **349**, 147–160 (2012).
- Alilain, W. J., Horn, K. P., Hu, H., Dick, T. E. & Silver, J. Functional regeneration of respiratory pathways after spinal cord injury. *Nature* **475**, 196–200 (2011).
- Massey, J. M. *et al.* Chondroitinase ABC digestion of the perineuronal net promotes functional collateral sprouting in the cuneate nucleus after cervical spinal cord injury. *J. Neurosci.* **26**, 4406–4414 (2006).
- Shen, Y. *et al.* PTP $\sigma$  is a receptor for chondroitin sulfate proteoglycan, an inhibitor of neural regeneration. *Science* **326**, 592–595 (2009).
- Coles, C. H. *et al.* Proteoglycan-specific molecular switch for RPTP $\sigma$  clustering and neuronal extension. *Science* **332**, 484–488 (2011).
- Bloechlinger, S., Karchewski, L. A. & Woolf, C. J. Dynamic changes in glypican-1 expression in dorsal root ganglion neurons after peripheral and central axonal injury. *Eur. J. Neurosci.* **19**, 1119–1132 (2004).
- Hsueh, Y. P. & Sheng, M. Regulated expression and subcellular localization of syndecan heparan sulfate proteoglycans and the syndecan-binding protein CASK/LIN-2 during rat brain development. *J. Neurosci.* **19**, 7415–7425 (1999).
- Matsuo, I. & Kimura-Yoshida, C. Extracellular modulation of Fibroblast growth factor signaling through heparan sulfate proteoglycans in mammalian development. *Curr. Opin. Genet. Dev.* **23**, 399–407 (2013).
- Inatani, M. & Yamaguchi, Y. Gene expression of EXT1 and EXT2 during mouse brain development. *Brain Res. Dev. Brain Res.* **141**, 129–136 (2003).
- Grimpe, B. & Silver, J. A novel DNA enzyme reduces glycosaminoglycan chains in the glial scar and allows microtransplanted dorsal root ganglia axons to regenerate beyond lesions in the spinal cord. *J. Neurosci.* **24**, 1393–1397 (2004).
- Oudega, M. *et al.* Systemic administration of a deoxyribozyme to xylosyltransferase-1 mRNA promotes recovery after a spinal cord contusion injury. *Exp. Neurol.* **237**, 170–179 (2012).
- McKillop, W. M., Dragan, M., Schedl, A. & Brown, A. Conditional Sox9 ablation reduces chondroitin sulfate proteoglycan levels and improves motor function following spinal cord injury. *Glia* **61**, 164–177 (2013).
- Tsuiji, O. *et al.* Therapeutic potential of appropriately evaluated safe-induced pluripotent stem cells for spinal cord injury. *Proc. Natl Acad. Sci. USA* **107**, 12704–12709 (2010).
- Uetani, N. *et al.* Mammalian motoneuron axon targeting requires receptor protein tyrosine phosphatases sigma and delta. *J. Neurosci.* **26**, 5872–5880 (2006).
- Kobayashi, S. *et al.* Association of EXT1 and EXT2, hereditary multiple exostoses gene products, in Golgi apparatus. *Biochem. Biophys. Res. Commun.* **268**, 860–867 (2000).
- Lairson, L. L., Henrissat, B., Davies, G. J. & Withers, S. G. Glycosyltransferases: structures, functions, and mechanisms. *Annu. Rev. Biochem.* **77**, 521–555 (2008).
- Mu, P. *et al.* Systemic delivery of siRNA specific to tumor mediated by atelocollagen: combined therapy using siRNA targeting Bcl-xL and cisplatin against prostate cancer. *Int. J. Cancer* **125**, 2978–2990 (2009).
- Wang, X. *et al.* Ibuprofen enhances recovery from spinal cord injury by limiting tissue loss and stimulating axonal growth. *J. Neurotrauma* **26**, 81–95 (2009).



53. Boato, F. *et al.* C3 peptide enhances recovery from spinal cord injury by improved regenerative growth of descending fiber tracts. *J. Cell Sci.* **123**, 1652–1662 (2010).
54. Lin, R., Kwok, J. C. F., Crespo, D. & Fawcett, J. W. Chondroitinase ABC has a long-lasting effect on chondroitin sulfate glycosaminoglycan content in the injured rat brain. *J. Neurochem.* **104**, 400–408 (2008).
55. Li, H. P. *et al.* Regeneration of nigrostriatal dopaminergic axons by degradation of chondroitin sulfate is accompanied by elimination of the fibrotic scar and glia limitans in the lesion site. *J. Neurosci. Res.* **85**, 536–547 (2007).
56. Yoshioka, N. *et al.* Small molecule inhibitor of type I transforming growth factor- $\beta$  receptor kinase ameliorates the inhibitory milieu in injured brain and promotes regeneration of nigrostriatal dopaminergic axons. *J. Neurosci. Res.* **89**, 381–393 (2011).
57. Kitagawa, H., Kinoshita, A. & Sugahara, K. Microanalysis of glycosaminoglycan-derived disaccharides labeled with the fluorophore 2-aminoacridone by capillary electrophoresis and high-performance liquid chromatography. *Anal. Biochem.* **232**, 114–121 (1995).

### Acknowledgements

We thank M. Nakamura, T. Yamashita, M. Abematsu and K. Nakashima for instruction and advice on the SCI experiments; T. Shirasawa and M.L. Tremblay for antibodies; and I. Hasegawa and Y. Tada-Kinoshita for technical assistance. Generation of the T1KO and T2KO mice was supported by the TOGONO support group from the MEXT of Japan, and some antibodies were produced by Everest Biotech Ltd. (Upper Heyford, UK) for its Antibody award. This work was supported in part by KAKENHI (#17023019, #22022040 and #24111515 to M.I., #23592161 and #24110503 to K.T. and #23700440 to S.H.O.), Project Promoting Grants from Niigata University to M.I. and Agri-Health Translational

Research Project support (#4300) from Ministry of the Agriculture, Forestry and Fisheries of Japan to K.T. Post-doctoral grants from JSPS supported N.Y. and Y.W.

### Author contributions

M.I. and K.T. designed the experiments, and analysed the data. Y. Watanabe, K.Oh, K.Od, T.S., M.Y. and K.S. produced the gene-targeted mice. N.Y., S.H.O., M.O., C.K., Y. Wada and H. Kawano developed the SCI model and performed the biochemical and the histological experiments. N.M. designed the siRNA sequences. M.N. and H.O. taught members of the lab the techniques necessary for the SCI model. S.M. and H. Kitagawa performed the quantitative analysis of CS and HS. M.I. wrote the paper, and in part, K.T. wrote the Methods section.

### Additional information

**Supplementary Information** accompanies this paper at <http://www.nature.com/naturecommunications>

**Competing financial interests:** The authors declare no competing financial interests.

**Reprints and permission** information is available online at <http://npg.nature.com/reprintsandpermissions/>

**How to cite this article:** Takeuchi, K. *et al.* Chondroitin sulphate *N*-acetylgalactosaminyl-transferase-1 inhibits recovery from neural injury. *Nat. Commun.* **4**:2740 doi:10.1038/ncomms3740 (2013).



This article is licensed under a Creative Commons Attribution 3.0 Unported Licence. To view a copy of this licence visit <http://creativecommons.org/licenses/by/3.0/>.